

# Discovery of the $^{151}\text{Eu}$ $\alpha$ decay

N. Casali<sup>1,2</sup>, S.S. Nagorny<sup>1,\*</sup>, F. Orio<sup>3</sup>, L. Pattavina<sup>1</sup>, J.W. Beeman<sup>5</sup>, F. Bellini<sup>3,4</sup>, L. Cardani<sup>3,4</sup>, I. Dafinei<sup>3</sup>, S. Di Domizio<sup>6</sup>, M.L. Di Vacri<sup>1</sup>, L. Gironi<sup>7,8</sup>, M.B. Kosmyna<sup>9</sup>, B.P. Nazarenko<sup>9</sup>, S. Nisi<sup>1</sup>, G. Pessina<sup>8</sup>, G. Piperno<sup>3,4</sup>, S. Pirro<sup>8</sup>, C. Rusconi<sup>8</sup>, A.N. Shekhovtsov<sup>9</sup>, C. Tomei<sup>3</sup>, and M. Vignati<sup>3</sup>

<sup>1</sup>*INFN - Laboratori Nazionali del Gran Sasso, I-67010 Assergi (AQ) - Italy*

<sup>2</sup>*Dipartimento di Scienze Fisiche e Chimiche, Università degli Studi dell'Aquila, I-67100 Coppito (AQ) - Italy*

<sup>3</sup>*INFN - Sezione di Roma I, I-00185 Roma - Italy*

<sup>4</sup>*Dipartimento di Fisica - Università di Roma La Sapienza, I-00185 Roma - Italy*

<sup>5</sup>*Lawrence Berkeley National Laboratory, Berkeley, California 94720, USA*

<sup>6</sup>*Dipartimento di Fisica, Università di Genova and INFN - Sezione di Genova, I-16146 Genova - Italy*

<sup>7</sup>*Dipartimento di Fisica, Università di Milano-Bicocca, Milano I-20126 - Italy*

<sup>8</sup>*INFN - Sezione di Milano Bicocca, Milano I-20126 - Italy and*

<sup>9</sup>*Institute for Single Crystals, National Academy of Sciences of Ukraine, 61001 Kharkov, Ukraine*

(Dated: May 19, 2019)

We report on the observation of the  $^{151}\text{Eu}$   $\alpha$  decay to the ground state of  $^{147}\text{Pm}$ . We measured a half-life of  $T_{1/2} = (4.62 \pm 0.95(\text{stat.}) \pm 0.68(\text{syst.})) \times 10^{18}$  y and a Q-value of  $1948.9 \pm 6.9$  keV, using a 6.15 g  $\text{Li}_6\text{Eu}(\text{BO}_3)_3$  crystal operated as scintillating bolometer.

PACS numbers: 23.60.+e, 29.40.Mc, 07.57.Kp

## I. INTRODUCTION

A new era in the investigation of rare  $\alpha$  decays has started in 2003 with the observation of the  $\alpha$  decay of  $^{209}\text{Bi}$  with a half-life  $T_{1/2} = 1.9 \times 10^{19}$  y exploiting the scintillating bolometer technique [1]. This technique offers new opportunities to search for rare nuclear processes.

The main advantage in the use of bolometers is the wide choice of detector materials, that allows one to investigate rare decays of nuclides, with excellent detection efficiency (the detector is made of the decay source). Moreover, high energy resolutions (of the order of per thousand [2]) are achieved exploiting this technology. When the bolometer is also an efficient scintillator then the simultaneous readout of the heat and light channels enables the identification of the particle nature, which thus leads to an abrupt background suppression. In case of a rare  $\alpha$  decay with energy transition lower than 2.6 MeV (one of the most intense and energetic natural  $\gamma$  emission), the experimental sensitivity is strongly limited by the background induced by environmental  $\beta/\gamma$  interactions in the absorber. By means of scintillating bolometers it is possible to identify the interacting particles, whether they are  $\alpha$ s,  $\beta$ s/ $\gamma$ s or neutrons. This peculiar feature allows to strongly reduce the background, therefore improving the detector sensitivity, and making possible the search for low energy  $\alpha$  decays, in almost background-free energy regions.

The potential of such an experimental approach is proved by recent experiments in which the  $\alpha$  decay

of  $^{180}\text{W}$  [3] and  $^{209}\text{Bi}$  to first excited level [4] were detected, and also in the search for  $\alpha$  decays of lead isotopes [5].

Natural europium consists of two isotopes:  $^{151}\text{Eu}$  (47.81%) and  $^{153}\text{Eu}$  (52.19%) [6]; both are potentially  $\alpha$  active with decay energies of  $Q_\alpha = 1964.9 \pm 1.1$  keV and  $Q_\alpha = 272.5 \pm 2.0$  keV [7], respectively. While the low  $Q_\alpha$  for  $^{153}\text{Eu}$  gives no hope for an experimental observation due to the extremely long expected half-life (more than  $10^{140}$  y as quoted in [8]), theoretical estimations on the  $^{151}\text{Eu}$  half-life lie in range of  $10^{17}$ - $10^{19}$  y [8], and such sensitivity levels can be achieved by scintillating bolometers.

The  $\alpha$  decay of europium isotopes has been recently investigated using a 370 g  $\text{CaF}_2:\text{Eu}$  low background scintillator [8], which contains Eu only as a dopant with mass fraction of just 0.5%. The authors of that paper mentioned the first indication of the  $\alpha$  decay of  $^{151}\text{Eu}$  nuclide to the ground state of  $^{147}\text{Pm}$  with a half-life of  $T_{1/2} = 5_{-3}^{+11} \times 10^{18}$  y. Nevertheless, due to the large statistical uncertainty, the authors preferred to report also a limit on the half-life of the process:  $T_{1/2} > 1.7 \times 10^{18}$  y at 68% C.L.

In this work we report a compelling experimental observation of the  $^{151}\text{Eu}$   $\alpha$  decay to the ground state of  $^{147}\text{Pm}$  daughter nuclide, using a 6.15 g  $\text{Li}_6\text{Eu}(\text{BO}_3)_3$  crystal (41.1% of Eu in mass) operated as scintillating bolometer.

## II. EXPERIMENTAL TECHNIQUE

The crystal was grown using the Czochralski technique in a platinum crucible under air atmosphere in accordance with the thermal conditions described

\* Corresponding author: sergey.nagorny@lngs.infn.it

in [9]. The stoichiometric mixture of initial reagents ( $\text{Li}_2\text{CO}_3$ ,  $\text{Eu}_2\text{O}_3$  and  $\text{B}_2\text{O}_3$ ) was used to synthesize the  $\text{Li}_6\text{Eu}(\text{BO}_3)_3$  charge by solid phase synthesis as described in [10].

The crystal used in this work has an irregular shape due to the compromise of having the largest possible mass combined with an acceptable crystal quality. For this reasons part of the crystal shows unpolished rounded edges. Moreover, the crystal shows some small cleavage planes as well as some tiny inclusions in part of the structure.

The working principle of a scintillating bolometer consists in measuring the temperature rise produced by the interaction of particles with the crystal absorber, which is operated at few mK temperatures. When an ionizing particle deposits energy in the crystal, a large portion of it is converted to heat, while the rest to scintillation light, which is recorded by another bolometer facing the crystal. The heat and light signals are both recorded as positive temperature variations by the temperature sensors on the main absorber and on the light detector, which is also operated as a bolometer. According to the nature of the interaction,  $\alpha$  and  $\beta/\gamma$  particles will generate different heat-to-light ratios for the same energy deposition.

The  $\text{Li}_6\text{Eu}(\text{BO}_3)_3$  crystal was operated in a dilution  $^3\text{He}/^4\text{He}$  refrigerator in the Gran Sasso underground laboratory of INFN. The crystal was held in position by means of a high-purity copper structure. Germanium Neutron Transmutation Doped thermistors (Ge-NTD) are used as temperature sensors. They are coupled to the  $\text{Li}_6\text{Eu}(\text{BO}_3)_3$  crystal and to the light detector (LD) by means of resin epoxy glue. In order to maximize the light collection efficiency, the crystal was surrounded by a reflecting foil (3M VM2002). The operational features of the LD, namely a high purity Ge wafer (diameter 44.5 mm and thickness 300  $\mu\text{m}$ ), are described in [11].

### III. DATA ANALYSIS

The detector was operated for 462.2 h. The  $\text{Li}_6\text{Eu}(\text{BO}_3)_3$  crystal and the LD have completely independent read-out. Detailed information on the cryogenic facility electronics, the data acquisition and processing can be found in [12–14].

The amplitude of the heat and light signals is energy-calibrated by means of known calibration sources. The scintillation light is calibrated using a permanent  $^{55}\text{Fe}$  X-ray source faced to the LD, assuming a linear dependence of the signal amplitude from the light energy. The heat channel is energy-calibrated using the  $Q_\alpha$ -value of the  $\alpha$  decays of the crystal induced by radioactive internal contaminations, with a second order polynomial

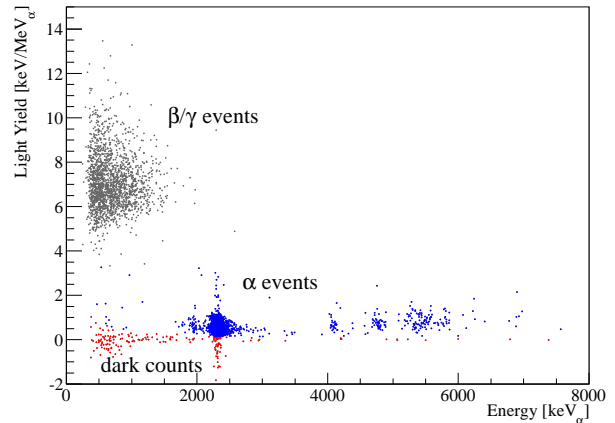


FIG. 1. Light Yield vs Heat scatter plot corresponding to 462.2 hours of background measurement with the 6.15 g  $\text{Li}_6\text{Eu}(\text{BO}_3)_3$  crystal. The heat channel is energy-calibrated using the  $Q_\alpha$  of the  $\alpha$  internal decays of the crystal (crystal contaminations). Three classes of events are identified, each one is characterized by a different Light Yield (LY). Colors are used to highlight the  $\alpha$  and the dark counts band.

with zero intercept.

In Fig. 1, the heat-to-light ratio (LY) is reported as a function of the heat deposited in the main crystal, for the acquired statistics of 462.2 h. The  $\beta/\gamma$  and the  $\alpha$  interactions in the detector are separated by the different LY, in agreement with the "Birks law" where  $\alpha$  interactions produce lower light signals compared to  $\beta/\gamma$  ones [15]. In the lower energy region of the scatter plot there is a continuum of events that does not produce light. These dark counts can be induced by several mechanisms. Firstly, a crystal with defects (like ours) can give rise to portions of volumes in which the scintillation process is strongly reduced. Secondly, a not-perfect crystal in which the structure is stressed by a not-homogeneous structure can give rise to sudden lattice relaxations resulting in thermal pulses without the emissions of photons. Finally, we have to take into account the ratio between the volumes of the Ge-NTD thermistor and the absorber scintillating crystal (roughly 1:600). A fraction of  $\beta/\gamma$  events will release energy inside the thermometer, thus producing a thermal signal without photon emission. In order to reject these events that produce an almost flat background in the region of interest, a cut on the absolute light signal is performed.

#### A. Alpha energy spectrum

Looking in Fig. 1, it is possible to reject  $\beta/\gamma$  events performing a cut on the heat-to-light ratio:  $\text{LY} < 3.3 \text{ keV/MeV}$  with a  $(99.99 \pm 0.01)\%$  rejection efficiency. To exclude dark counts, we selected events with

detected light higher than 0.4 keV with an efficiency of  $(96.8 \pm 0.2)\%$ . The obtained energy spectrum is shown in

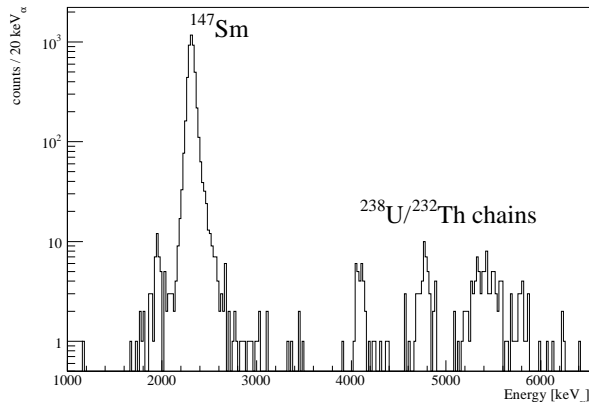


FIG. 2. Alpha energy spectrum for the entire collected statistics with the 6.15 g  $\text{Li}_6\text{Eu}(\text{BO}_3)_3$  crystal during 462.2 hours. The events are selected applying two cuts on the light channel. The events are attributed to internal contaminations of the crystal, the most intense one is the  $^{147}\text{Sm}$   $\alpha$  decay at 2311 keV, while the peaks above 4 MeV relate to  $\alpha$  decays of daughter nuclides from  $^{238}\text{U}/^{232}\text{Th}$  chains.

Fig. 2. The most prominent peak in the energy spectrum is due to an internal contamination of Sm, namely  $^{147}\text{Sm}$  with an activity of 454 mBq/kg. In the high energy region, above 4 MeV, there are peaks produced by  $^{232}\text{Th}$  decay chain products, at a level of 3.5 mBq/kg, and  $^{238}\text{U}$  chain daughter nuclides such as  $^{226}\text{Ra}$  and  $^{210}\text{Po}$  with activities of 2.9 mBq/kg and 6.2 mBq/kg, respectively. The most intense internal contaminations were used for the calibration of the  $\alpha$  energy spectrum, namely  $^{147}\text{Sm}$  (2311 keV),  $^{232}\text{Th}$  (4083 keV) and  $^{226}\text{Ra}$  (4871 keV). The mis-calibration level at 2311 keV ( $^{147}\text{Sm}$   $\alpha$  decay) is less than 1 keV.

In the energy spectrum in Fig. 2, on the left side of the  $^{147}\text{Sm}$  line there is a clear peak in the 1900-2000 keV window. As will be shown in the following, we interpret this peak as being produced by the  $\alpha$  decay of  $^{151}\text{Eu}$ . At energies lower than 1900 keV and larger than 2000 keV there is no flat background, induced by surface contaminations [16]. Thus, the only background in our region of interest is produced by  $^{147}\text{Sm}$ .

According to our knowledge there are three  $\alpha$  active nuclides which could mimic or spoil our observed signal, having energy transitions close to the  $^{151}\text{Eu}$  Q-value. They are  $^{144}\text{Nd}$  ( $Q = 1905 \pm 1$  keV,  $T_{1/2} = 2.3 \times 10^{15}$  y),  $^{148}\text{Sm}$  ( $Q = 1986 \pm 1$  keV,  $T_{1/2} = 7.0 \times 10^{15}$  y) and  $^{152}\text{Gd}$  ( $Q = 2203.0 \pm 1.4$  keV,  $T_{1/2} = 1.1 \times 10^{14}$  y). The concentration of these elements in the crystal was determined using a High Resolution Inductively Coupled Plasma-Mass Spectrometric (HR-ICP-MS) analysis. The obtained results are  $4.9 \times 10^{-6}$  g/g,  $4.7 \times 10^{-6}$  g/g and

$91.3 \times 10^{-6}$  g/g for Nd, Sm and Gd elements. These values correspond to just 0.5, 0.1 and 1.5 events over the live time of the measurement for  $^{144}\text{Nd}$ ,  $^{148}\text{Sm}$  and  $^{152}\text{Gd}$   $\alpha$  decay, respectively. The robustness of these results is demonstrated by the HR-ICP-MS measurement. In fact, the measured concentration of the Sm element, scaled for the natural isotopic abundance of  $^{147}\text{Sm}$ , is in agreement with the computed activity with an error of 15%.

## B. Response function and discovery significance

The observed response function (RF) of the  $\text{Li}_6\text{Eu}(\text{BO}_3)_3$  bolometer for  $\alpha$  particles is not gaussian. This feature is visible looking at the  $^{147}\text{Sm}$  peak (Fig. 2). We do not have a clear explanation for the non-Gaussian shape of the  $^{147}\text{Sm}$   $\alpha$  peak. We can speculate that the phonon collection was spoiled by cracks in the crystal. This led to a worsening of the detector energy resolution and also affected the detector response function.

The RF that better describes the peak with the largest statistics is the sum of two Crystal Ball (CB) functions [17] with the same mean ( $Q_\alpha$ -value), one with a left tail and one with a right tail:  $\text{RF}(Q, E) = N \cdot [\text{CB}_{\text{left}}(Q, E) + \delta \cdot \text{CB}_{\text{right}}(Q, E)]$ , where  $N$  is the number of events in the peak and  $\delta$  the ratio between the two CB functions. The shape of the response function evaluated on the  $^{147}\text{Sm}$  peak is shown in Fig. 3.

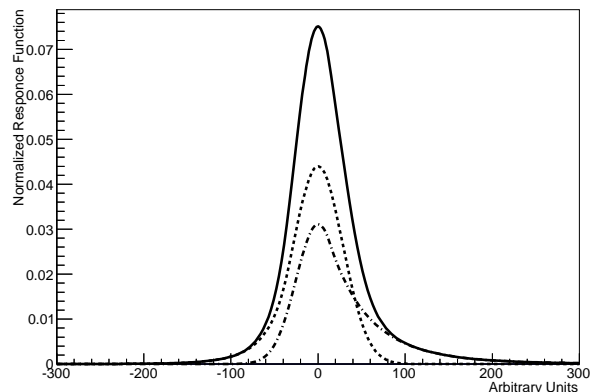


FIG. 3. Normalized response function of the detector for interacting  $\alpha$  particles in the  $\text{Li}_6\text{Eu}(\text{BO}_3)_3$  crystal. The dashed lines represent the two Crystal Ball functions, while the solid one is the sum of the two components.

Once the response function of the bolometer for  $\alpha$  particles is defined, it is possible to perform a fit in the  $\alpha$  energy spectrum, in order to evaluate the number of  $^{151}\text{Eu}$  events. The fit function (FF) used is:

$$\text{FF}(E) = N_{\text{Sm}} \cdot \text{RF}(Q_{\text{Sm}}, E) + N_{\text{Eu}} \cdot \text{RF}(Q_{\text{Eu}}, E) \quad (1)$$

where  $N_{\text{Sm}}$  and  $N_{\text{Eu}}$  are the number of events in the  $^{147}\text{Sm}$  and  $^{151}\text{Eu}$  peaks (free parameters of the fit). Furthermore, the  $^{147}\text{Sm}$  Q-value is constrained at its value [7], while the  $^{151}\text{Eu}$  one is left as a free parameter.

In Fig. 4, the fitted  $\alpha$  energy spectrum from 1.2 MeV to 4 MeV is shown. The number of  $^{151}\text{Eu}$  events

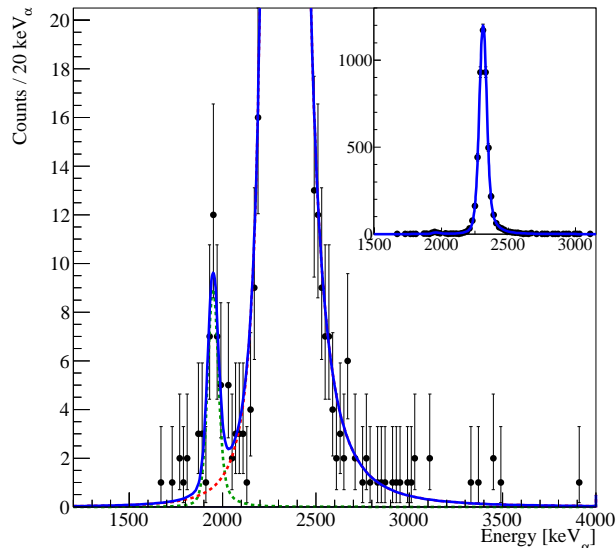


FIG. 4. Zoom of the  $\alpha$  energy spectrum around the region of interest. Two peaks are visible:  $^{147}\text{Sm}$  at 2311 keV and  $^{151}\text{Eu}$  at 1649 keV, in the inset the full y-scale plot is shown. The response function of the detector is assumed to be the sum of two Crystal Ball functions and this is used for fitting the two observed peaks in the  $\alpha$  energy spectrum. The dashed lines represent the detector response function, while the solid line is the sum of the response function of the two peaks.

( $N_{\text{Eu}}$ ) which maximizes the unbinned and extended likelihood, corrected for the event selection efficiency evaluated on the  $^{147}\text{Sm}$  peak ( $96.8 \pm 0.2\%$ ), is equal to  $37.6 \pm 7.5$  counts. The measured Q-value for the  $^{151}\text{Eu}$   $\alpha$  transition is  $1948.9 \pm 6.9$  keV, and the FWHM energy resolution is  $65 \pm 7$  keV.

In order to quantify the statistical significance of an excess over the background-only expectation ( $^{147}\text{Sm}$  induced background) it is possible to define the test statistic  $q_0$  with the same method adopted in [18]:

$$q_0 = -2 \cdot \ln \frac{L(\text{data} \mid \text{bkg}(\hat{\theta}_0))}{L(\text{data} \mid \hat{\mu} \cdot \text{signal}(\hat{\theta}) + \text{bkg}(\hat{\theta}))} \quad (2)$$

where  $\hat{\theta}_0$  and  $\hat{\theta}$  are the fit parameter values that maximize the likelihood, in the background-only hypothesis ( $\hat{\theta}_0$ ) and in the background plus signal hypothesis ( $\hat{\theta}$ ). While  $\hat{\mu}$  is the number of signal events that maximizes the likelihood. Given these definitions, a signal-like excess, i.e.  $\mu > 0$ , corresponds to a positive value of  $q_0$ .

In the absence of an excess,  $\mu = 0$ , the likelihood ratio is equal to one, and  $q_0$  is zero; the excess of events that we observed gives  $q_0 = 54$ , corresponding to a  $7.4 \sigma$  statistical significance. Therefore the probability that the measured excess of events is produced by a background fluctuation is of the order of  $10^{-14}$ .

#### IV. $^{151}\text{Eu}$ HALF-LIFE

The number of  $^{151}\text{Eu}$  atoms in the 6.15 g  $\text{Li}_6\text{Eu}(\text{BO}_3)_3$  crystal is  $(4.76 \pm 0.07) \times 10^{21}$ , evaluated taking into account the measured isotope composition of Eu measured with HR-ICP-MS ( $47.6 \pm 0.7\%$ ). This measurement allows to minimize the systematic uncertainty in the evaluation of the  $^{151}\text{Eu}$  half-life value. The choice of the fit interval and of the fit function causes a variation on the estimated number of  $^{151}\text{Eu}$  events. For example, shrinking the fit range (1800-2800 keV), causes a reduction of  $^{151}\text{Eu}$  events of 5.3 counts, while changing the response function to a CB + a Gaussian increases the number of  $^{151}\text{Eu}$  events by 0.9 counts. Finally, we neglect the mis-calibration error because of the small value compared to the detector energy resolution.

Considering the observed number of events corrected for the event selection efficiency ( $37.6 \pm 7.5$  counts), the containment efficiency of  $^{151}\text{Eu}$   $\alpha$  decay evaluated by means of Monte Carlo simulations ( $\epsilon = 99.98\%$ ) and the live time of the measurement (462.2 h), we obtain the following value for the half-life of  $^{151}\text{Eu}$  to the ground state of  $^{147}\text{Pm}$  daughter nuclide:

$$T_{1/2} = (4.62 \pm 0.95(\text{stat.}) \pm 0.68(\text{syst.})) \times 10^{18} \text{ y.} \quad (3)$$

This value is in agreement with previous experimental results reported in [8], and in accordance with theoretical calculations using several semi-empirical models [19–21].

#### V. CONCLUSION

In this work we reported on the discovery of  $^{151}\text{Eu}$   $\alpha$  decay to ground state of  $^{147}\text{Pm}$  with a measured half-life of  $T_{1/2} = (4.62 \pm 0.95(\text{stat.}) \pm 0.68(\text{syst.})) \times 10^{18} \text{ y}$  with a  $7.4 \sigma$  statistical significance.

The evaluated Q-value for the decay is  $1948.9 \pm 6.9$  keV. This result was obtained using a Eu-based crystal, such as  $\text{Li}_6\text{Eu}(\text{BO}_3)_3$ , operated as scintillating bolometer.

#### ACKNOWLEDGEMENTS

This project was supported by the Italian Ministry of Research under the PRIN 2010-2011 grant. This work was also supported by the ISOTTA project, funded within the ASPERA 2nd Common Call for R&D

Activities. Part of the work was carried out thanks to LUCIFER Project, funded by the European Research Council (FP7/2007-2013) grant agreement no. 247115.

Thanks are due to the LNGS mechanical workshop and

in particular to E. Tatananni, A. Rotilio, A. Corsi, and B. Romualdi for continuous and constructive help in the overall set-up construction. Finally, we are especially grateful to M. Perego and M. Guetti for their invaluable help.

- 
- [1] P. de Marcillac *et al.*, *Nature* **422**, 876 (2003).
  - [2] J. Beeman *et al.*, *Eur. Phys. J. C* **72**, 2142 (2012).
  - [3] C. Cozzini *et al.*, *Phys. Rev. C* **70**, 064606 (2004).
  - [4] J. Beeman *et al.*, *Phys. Rev. Lett.* **108**, 062501 (2012).
  - [5] J. Beeman *et al.*, *Eur. Phys. J. A* **49**, 50 (2013).
  - [6] M. Berglund and M.E. Wieser, *Pure Appl. Chem.* **83**, 397 (2011).
  - [7] G. Audi *et al.*, *Nucl. Phys. A* **729**, 337 (2003).
  - [8] P. Belli *et al.*, *Nucl. Phys. A* **789**, 15 (2007).
  - [9] V.N. Baumer *et al.*, *J. Cryst. Growth* **242**, 167(2002).
  - [10] B.V. Grinyov *et al.*, Patent UA 66072 (2003).
  - [11] J. Beeman *et al.*, *J. Instrum.* **8**, P05021 (2013).
  - [12] S. Pirro *et al.*, *Nucl. Instrum. Meth. A* **444**, 331 (2000).
  - [13] C. Arnaboldi *et al.*, *Nucl. Instrum. Meth. A* **520**, 578 (2002).
  - [14] G. Piperno *et al.*, *J. Instrum.* **6**, P10005 (2011).
  - [15] J.B. Birks, *Proc. Phys. Soc. A* **64**, 874 (1951).
  - [16] M. Clemenza *et al.*, *Eur. Phys. J. C* **71**, 1805 (2011).
  - [17] J.E. Gaiser, Report SLAC-R-255 p178 (1982).
  - [18] CMS Collaboration, *Phys. Lett. B* **710**, 26 (2012).
  - [19] D.N. Poenaru and M. Ivascu, *J. Phys.* **44**, 791 (1983).
  - [20] D.N. Poenaru *et al.*, *Phys. Rev. C* **32**, 2198 (1985).
  - [21] O.A.P. Tavares and E.L. Medeiros, *Phys. Scr.* **76**, 163 (2007).